References

ABAD-ZAPATERO, C., ABDEL-MEGUID, S. S., JOHNSON, J. E., LESLIE, A. G. W., RAYMENT, I., ROSSMANN, M. G., SUCK, D. & TSUKIHARA, T. (1980). *Nature (London)*, **286**, 33–39.

ABAD-ZAPATERO, C., ABDEL-MEGUID, S. S., JOHNSON, J. E., LESLIE, A. G. W., RAYMENT, I., ROSSMANN, M. G., SUCK, D. & TSUKIHARA, T. (1981). *Acta Cryst.* B**37**, 2002–2018.

ARGOS, P., FORD, G. C. & ROSSMANN, M. G. (1975). *Acta Cryst.* A**31**, 499–506.

BLOOMER, A. C., CHAMPNESS, J. N., BRICOGNE, G., STADEN, R. & KLUG, A. (1978). *Nature (London)*, **276**, 362–368.

BRICOGNE, G. (1974). *Acta Cryst.* A**30**, 395–405.

BRICOGNE, G. (1976). *Acta Cryst.* A**32**, 832–847.

CASPAR, D. L. D. & KLUG, A. (1962). *Cold Spring Harbor Symp. Quant. Biol.* **27**, 1–24.

FINCH, J. T. (1974). *J. Gen. Virol.* **24**, 359–364.

HARRISON, S. C. (1971). *Cold Spring Harbor Symp. Quant. Biol.* **36**, 495–501.

HARRISON, S. C. & JACK, A. (1975). *J. Mol. Biol.* **97**, 173–191.

HARRISON, S. C., OLSON, A. J., SCHUTT, C. E., WINKLER, F. K. & BRICOGNE, G. (1978). *Nature (London)*, **276**, 368–373.

JOHNSON, J. E. (1978). *Acta Cryst.* B**34**, 576–577.

JOHNSON, J. E., AKIMOTO, T., SUCK, D., RAYMENT, I. & ROSSMANN, M. G. (1976). *Virology*, **75**, 394–400.

MAIN, P. (1967). *Acta Cryst.* **23**, 50–54.

NORDMAN, C. E. (1980). *Acta Cryst.* A**36**, 747–754.

RAYMENT, I., BAKER, T. S., CASPAR, D. L. & MURAKAMI, W. T. (1982). *Nature (London)*, **295**, 110–115.

ROSSMANN, M. G. (1972). *The Molecular Replacement Method.* New York: Gordon and Breach.

ROSSMANN, M. G. & BLOW, D. (1962). *Acta Cryst.* **15**, 24–31.

UNGE, T., LILJAS, L., STRANDBERG, B., VAARA, I., KANNAN, K. K., FRIDBORG, K., NORDMAN, C. E. & LENTZ, P. J. JR (1980). *Nature (London)*, **285**, 373–377.

Acta Cryst. (1983). A**39**, 116–122

Effect of Dislocation Density on Integrated Intensity of X-ray Scattering by Silicon Crystals in Laue Geometry

BY N. M. OLEKHNOVICH, A. L. KARPEI, A. I. OLEKHNOVICH AND L. D. PUZENKOVA

Institute of Physics of Solids and Semiconductors, Byelorussian Academy of Sciences, Minsk 220726, *USSR*

(*Received* 29 *March* 1982; *accepted* 16 *August* 1982)

Abstract

An investigation of integrated intensity is performed for reflections 111 and 333 in plane-polarized Cu $K\alpha_1$ radiation for a series of silicon dislocation single crystals. Integrated intensity thickness oscillations (*Pendellösung* effect) have been found at low dislocation density (10–100 mm^{-2}). It is shown that the oscillations attenuate with increasing dislocation density, while their period somewhat increases. Thickness dependence of both extinction factor and polarization ratio is derived at high dislocation density (10^3–10^6 mm^{-2}). The present theoretical approaches based on the Darwin transfer equations appeared to be unsuitable for treating the obtained experimental data. They are analysed on the basis of coherent and diffuse scattering components.

1. Introduction

The previous investigations of polarization properties of Bragg reflections for silicon and germanium dislocation crystals (Olekhnovich, Markovich & Olekhnovich, 1980) show that the mosaic model of crystals is applicable for describing diffraction in real crystals, provided the dislocation density is over 10^4 mm^{-2}. Besides, diffraction in mosaic crystals is found to be practically determined only by primary extinction.

Kato (1980*a*,*b*), using equations of Takagi–Taupin type (Takagi, 1969), developed a statistical dynamical diffraction theory for crystals of any perfection degree. In this theory extinction is not subdivided into primary and secondary.

To establish the scattering mechanism of X-rays in real crystals it is important to study diffraction properties as a function of sample thickness using the Laue method. That method, as is known, allows one to investigate the *Pendellösung* effect, anomalous transmission, as well as the extinction effect. Lawrence & Mathieson (1977) proposed a simple method of single-crystal sample inclination for a controllable change of X-ray path length in Laue geometry. This procedure was used for studying integrated intensity thickness oscillation in perfect crystals (Somenkov, Shilstein, Belova & Utemisov, 1978).

The aim of the present work is to investigate the integrated intensity of X-ray scattering by silicon-containing dislocations in a symmetrical Laue case varying their thickness in the scattering plane. A thickness oscillation effect of integrated intensity was found at a small dislocation density while at a higher one, over 10^3 mm^{-2}, extinction factor and polarization ratio as a function of crystal thickness were determined.

The experimental data were analysed on the basis of the existing theories of diffraction in real crystals.

2. Experimental procedure

The measurements were made on silicon single-crystal plane-parallel wafers, cut out parallel to {110}. The wafer surfaces were mechanically polished and then etched chemically. Six samples with dislocation density from 10 to 10^6 mm^{-2} were prepared from non-doped single crystals having a uniform dislocation distribution. The wafer thicknesses, defined with an accuracy of 0·5 μm, were 62–107 μm.

Integrated intensities of 111 and 333 reflections were measured in Cu $K\alpha_1$ plane-polarized radiation using a double-crystal Bragg–Laue spectrometer. A perfect germanium crystal (reflection 333) served as monochromator. Incident monochromatic beam intensity was measured by means of an attenuating filter, which was the sample under study. The polarization ratio ρ_π/ρ_σ was defined by measuring the integrated intensity for π and σ polarizations of the incident beam. Effective crystal thickness $t = t_0/\cos\varphi$ was varied by tilting the sample around the reciprocal-lattice vector (Lawrence & Mathieson, 1977). Here t_0 is the thickness of the plane-parallel plate, φ is its tilt angle. The latter changed from 0 to ±75°. The integrated intensity values, measured at two similar tilt angles φ and $-\varphi$ proved to be close to each other and the mean values were used in further analyses. No correction was applied for TDS, since it did not exceed the error of the measured intensity.

3. Results and analyses

The measurements show that the integrated-intensity change with effective crystal thickness depends on dislocation density. Figs. 1 and 2 give the factor $Y = \rho/\rho_K$ as a function of the effective crystal thickness for the reflections 111 and 333, respectively. Here ρ is the integrated intensity measured for σ polarization of the incident beam; ρ_K is the integrated intensity for thickness t in the kinematical limit. In calculating ρ_K the structure and the Debye–Waller factors were taken from Aldred & Hart's (1973) data. The photoelectric absorption coefficient was assumed to be 140 cm^{-1}.

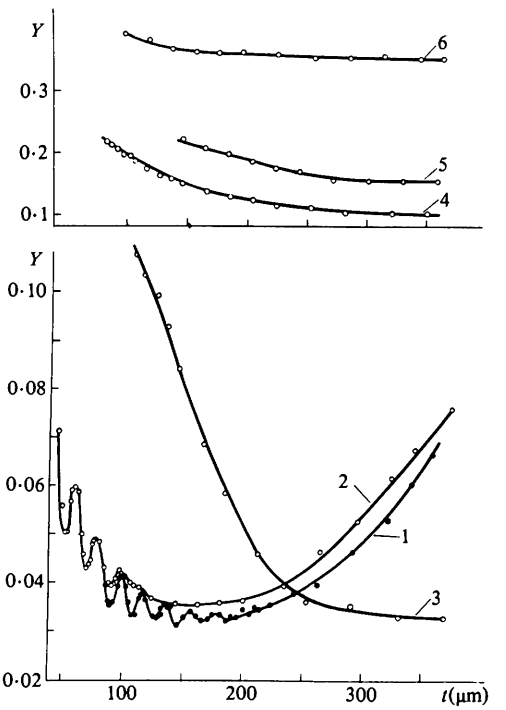

Fig. 1. Thickness dependence of the ratio ρ/ρ_K for reflection 111 at dislocation density (1) 30; (2) 100; (3) $7{\cdot}5 \times 10^3$; (4) $4{\cdot}8 \times 10^4$; (5) $1{\cdot}3 \times 10^5$; (6) 10^6 mm^{-2}.

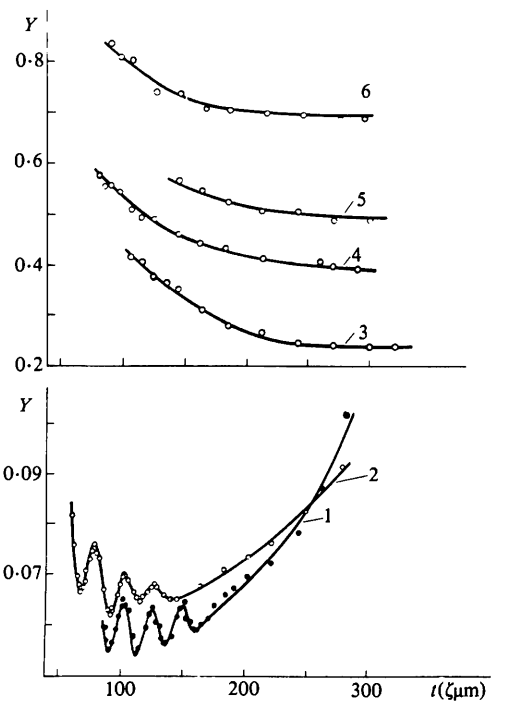

Fig. 2. Thickness dependence of the ratio ρ/ρ_K for reflection 333 at different dislocation densities (same symbols as in Fig. 1).

As the figures show, the integrated intensity dependence on the effective crystal thickness for samples I and II [having dislocation densities (N_d) of 30 and 100 mm^{-2} (curves 1, 2)] differs qualitatively from that for samples III–VI [with N_d $7{\cdot}5 \times 10^3$, $4{\cdot}8 \times 10^4$, $1{\cdot}3 \times 10^5$ and 1×10^6 mm^{-2}, respectively (curves 3–6)]. For the first group of samples integrated intensity oscillations are apparent when the values of effective crystal thickness are small. The oscillations attenuate both with increasing effective crystal thickness and with dislocation density. The absolute value of the integrated intensity in this range of crystal thickness increases with the dislocation density.

Effective crystal thickness lying beyond the range of the *Pendellösung* fringes, the factor Y increases smoothly due to the anomalous transmission effect. Intersection of the curves 1 and 2 in Fig. 2 reveals that the rate at which the Y factor increases slows down with the dislocation density.

Neither oscillations nor an anomalous transmission effect occur for samples III–VI. In this case extinction takes place. It is of interest that the extinction factor as a function of effective crystal thickness tends to a constant. The higher the dislocation density is, the smaller should be the effective thickness for the extinction factor to reach the limit value.

The polarization ratio for all studied samples (Fig. 3) within the experimental error does not depend on the effective crystal thickness. It exceeds unity for the sample 111 with the dislocation density $7{\cdot}5 \times 10^3$ mm^{-2} (curve 1), *i.e.* $\rho_\pi > \rho_\sigma$. As the dislocation density increases the polarization ratio goes down, approaching the kinematical limit ($\cos^2 2\theta_B$).

First of all let us analyse the experimental data for samples I and II (cases of low dislocation density) and then for the III–VI samples (cases of high dislocation density).

Cases of low dislocation density

According to Kato's (1980*b*) theory the integrated intensity for a real crystal in the symmetrical Laue case is given by

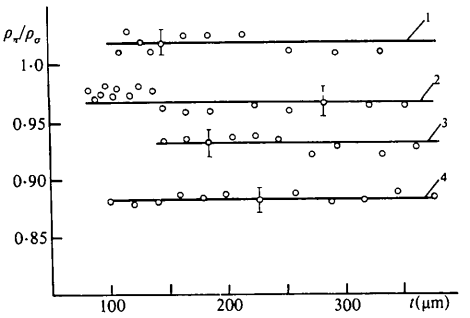

Fig. 3. Polarization ratio for reflection 111 *vs* crystal thickness at various dislocation densities: (1) $7{\cdot}5 \times 10^3$; (2) $4{\cdot}8 \times 10^4$; (3) $1{\cdot}3 \times 10^5$; (4) 10^6 mm^{-2}.

$$\rho = R_g^c + R_g^{ca} + R_g^i + R_g^m, \tag{1}$$

where

$$R_g^c + R_g^{ca} = \frac{\rho_K E}{2A} \exp[-2(1-E^2)\,\tau A/\Lambda] \times \left[\int_0^{2AE} \mathcal{J}_0(x)\,dx + I_0(2kAE) - 1\right] \tag{2}$$

is the purely coherent component, R_g^i and R_g^m are the incoherent and mixed components [equations (29*b*) and (36*b*) of Kato (1980*b*)], $A = t/\Lambda\gamma$, $\Lambda = v/r_0\lambda|F'|C$, $\gamma = \cos\theta_B$, $k = F''/F'$, E is a static Debye–Waller factor, τ is the correlation length.

For crystals with low dislocation density, as will be seen below, the condition of 'nearly perfect crystal' is fulfilled (Kato, 1980*b*). Therefore, for calculating R_g^{ca} we used the exact expression (Kato, 1968), where the structure factor is corrected by the static Debye–Waller factor E.

The incoherent and the mixed components in (1) are determined by the static Debye–Waller factor E and the effective correlation length τ_e. The latter, taking into account Kato's (1980*a*, p. 769) remark, is defined by

$$\tau_e = (1-E^2)\,\tau + bE\Lambda,$$

where b is a numerical factor of order unity. Kato in his calculations takes $b = 1$. While comparing our experiment with the theory we varied this factor.

The reduced value of the integrated intensity was defined to compare the experimental data with theoretical ones

$$R_{r\,\mathrm{exp}} = 2A\rho/\rho_K - [I_0(2kAE) - 1] \times E\exp[-2(1-E^2)\,\tau A/\Lambda], \tag{3}$$

$$R_{r\,\mathrm{th}} = (2A/\rho_K)\,(R_g^c + R_g^i + R_g^m). \tag{4}$$

The factor E was determined directly from the period of the integrated intensity oscillations. The estimations show that for the reflection 333 $E = 0{\cdot}99$ at $N_d = 30$ mm^{-2} (sample I), and $E = 0{\cdot}97$ at $N_d = 100$ mm^{-2} (sample II). The increase in oscillation period for reflection 111 of sample II is less than 1%.

The parameter τ was evaluated by the ratio of the first oscillation amplitude for the real crystal to the amplitude of the corresponding oscillation for the perfect one. For example, for reflection 333 (sample II) $\tau = 0{\cdot}204\Lambda$. Fig. 4 shows that the experimental value of R_r (curve 1) is much larger than the theoretical one (curve 2) over all the range of the effective crystal thickness variation. At the same time oscillations of $R_{r\,\mathrm{exp}}$ damp very quickly compared to $R_{r\,\mathrm{th}}$. The value of $R_{r\,\mathrm{th}}$ depends weakly on the factor b in the expression for τ_e. For example, $R_{r\,\mathrm{th}}$ increases only by about 1·5% with the factor varying from 1 to 2.

The $R_{r\,\mathrm{exp}}$ and $R_{r\,\mathrm{th}}$ behaviour for reflection 111 is similar to that for reflection 333.

Let us analyse the experimental data from the point of view of coherent and diffuse scattering parts (Dederichs, 1970; Lider, Chukhovskii & Roganskii, 1977). The latter component in our case is the scattering due to the fields of dislocation lattice deformation. It makes a contribution mainly to the Bragg reflection regions (Krivoglaz, 1967) and manifests itself in rocking-curve broadening and some intensity increase on their tails. One can assume that the diffuse scattering causes coherent scattering absorption as in the case for other statistical distributed defects (Dederichs, 1970). Besides, in the region of the Bragg reflection the diffuse scattering attenuates due to extinction effect. Then the integrated intensity could be determined as

$$\rho = \rho_K(1-E^2)\,Y_d + \frac{\rho_K E}{2A}\exp\left(-\frac{\mu_d t}{\gamma}\right) \times \left[\int_0^{2AE} \mathscr{J}_0(x)\,dx + I_0(2kAE) - 1\right], \quad (5)$$

where μ_d is the absorption coefficient because of diffuse scattering, Y_d is the integrated extinction factor of the diffuse scattering.

The coefficient μ_d was found in the same way as the parameter τ in (2). It appeared to be equal to about 8·3 and 22·1 cm^{-1} for reflection 333 of samples I and II, respectively.

Subtracting

$$(\rho_K E/2A)\exp(-\mu_d t/\gamma) I_0(2kAE)$$

from the experimental value of ρ and smoothing the oscillations, we define the reduced intensity of the diffuse scattering (Fig. 5, curve 2). Its calculated value is given by

$$R_{rd} = 2A(1-E^2)\,Y_d. \quad (6)$$

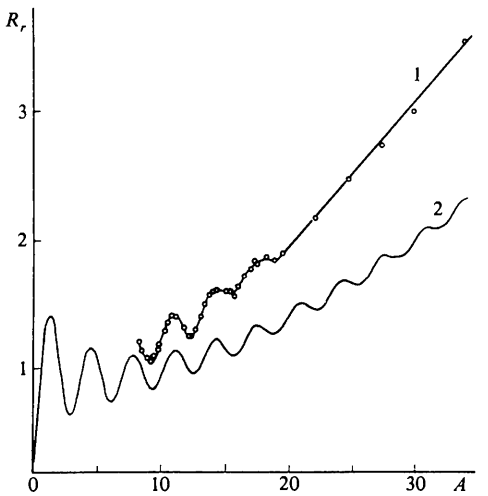

Fig. 4. The reduced intensity of reflection 333 *vs* parameter A: (1) experimental; (2) calculated from equation (4) ($b = 1$).

Fig. 5 gives for comparison the thickness dependence R_{rd}, calculated in the kinematical limit [$Y_d = 1$ in (6)] (dashed line 1) and also the sum of the reduced values for incoherent and mixed components contained in equation (1) (curve 3). To calculate the latter, the parameter τ was found from the relation $2(1-E^2)\,\tau/A = \mu_d A$. Comparison of the given data in Fig. 5 suggests that the found value of R_{rd} (curve 2) can be explained on the basis of (6) taking into account extinction factors of the diffuse scattering.

Consequently, using the approach based on coherent and diffuse scattering components, one can treat more correctly the observed thickness dependence of the integrated intensity for crystals with low dislocation density. However, it should be pointed out that (5) as well as (2) cannot quantitatively account for the effect of quick damping of the integrated intensity thickness oscillations for dislocation crystals. This effect is, apparently, due to an additional phase difference for the coherent waves in such crystals.

Cases of high dislocation density

As dynamical effects do not appear for the crystals having high dislocation density, the integrated intensity from Kato's (1980*b*) theory is determined only by the incoherent scattering component. The extinction factor in this case for σ polarization can be written as

$$Y = \frac{1}{at}[1-\exp(-at)], \quad (7)$$

where

$$a = 4\tau/A^2\gamma.$$

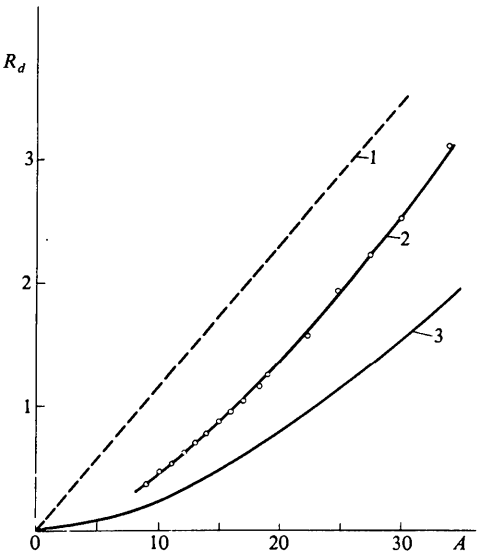

Fig. 5. The reduced diffuse component intensity: (1) calculated from the kinematical theory; (2) experimental; (3) calculation of $R_s^i + R_s^m$ (equation 1).

To compare with the experimental data we transform (7) to

$$\ln[\mathrm{d}(Yt)/\mathrm{d}t] = -at. \tag{8}$$

This is the equation of a straight line, passing through the origin (Fig. 6, dashed lines).

At $a_\pi = C^2 a_\sigma$, the polarization ratio is given by

$$\rho_\pi/\rho_\sigma = \frac{1-\exp(-C^2 a_\sigma t)}{1-\exp(-a_\sigma t)}. \tag{9}$$

Fig. 6 demonstrates the dependence of $-\ln[\mathrm{d}(Yt)/\mathrm{d}t]$ on the crystal thickness from the experimental data for the reflections 111 and 333 (for reflection 111 of sample III $\mathrm{d}(Yt)/\mathrm{d}t < 0$).

It is seen that the thickness dependence of $-\ln[\mathrm{d}(Yt)/\mathrm{d}t]$, following from (8), does not agree even qualitatively with the experimental one.

The same thing is inherent in the thickness dependence of the polarization ratio (Fig. 7). According to (9) the polarization ratio should change from $\cos^2 2\theta_B$ (at $t \to 0$) to 1 (curve 3) for any degree of crystal imperfection. The experiment indicates that practically it does not depend on crystal thickness and at a certain dislocation density it may exceed unity. This suggests that Kato's theory is not suitable for describing diffraction in real crystals.

Let us turn to Zachariasen's (1967) theory of the secondary extinction (1967). For the symmetrical Laue case the transfer equations have the exact solution, from which the extinction factor can be found for a given mosaic type.

For the Gaussian distribution of the blocks (Becker & Coppens, 1974) the extinction factor can be defined by

$$Y = Y_p \sum_{n=1} \frac{(-1)^{n+1}}{\sqrt{n}\,n!} \left(\frac{2a_G Q Y_p t}{\cos\theta_B}\right)^{n-1}. \tag{10}$$

At $2a_G Q Y_p t/\cos\theta_B \lesssim 1$ the series (10) can be approximated by

$$Y = Y_p \exp(-\alpha Q Y_p t). \tag{11}$$

The experimental data (Fig. 8) show the presence of a region in which the crystal thickness change of $\ln Y$ is given by a straight line as follows from (11). The straight-line intersection with the Y axis gives the value of the primary extinction factor. Its tilt-angle tangent defines the additional absorption coefficient of the diffracted radiation.

It is seen from Fig. 8 that an increase of the dislocation density leads to a decrease in the tilt angle of the linear part $\ln Y$ for both reflections. As regards the secondary extinction (11), this means a decrease in the value $\alpha Q Y_p$. The latter should lead to the elongation of the thickness region, where $\ln Y$ would change linearly. In reality it is quite the reverse, *i.e.* the region of linearly changing $\ln Y$ becomes shorter. The same discrepancy occurs when comparing the data for reflections 111 and 333 of the same sample. For example, in the case when $N_d = 7{\cdot}5 \times 10^3$ mm^{-2} the

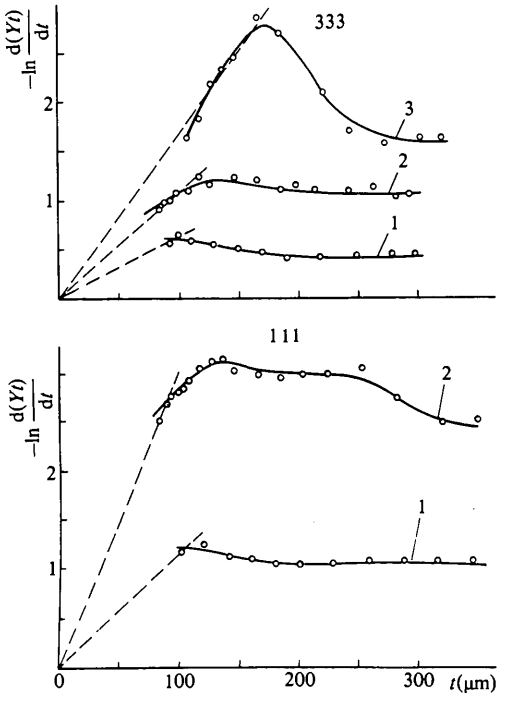

Fig. 6. $-\ln[\mathrm{d}(Yt)/\mathrm{d}t]$ *versus* crystal thickness at dislocation density (1) 10^6; (2) $4{\cdot}8 \times 10^4$; (3) $7{\cdot}5 \times 10^3$ mm^{-2}.

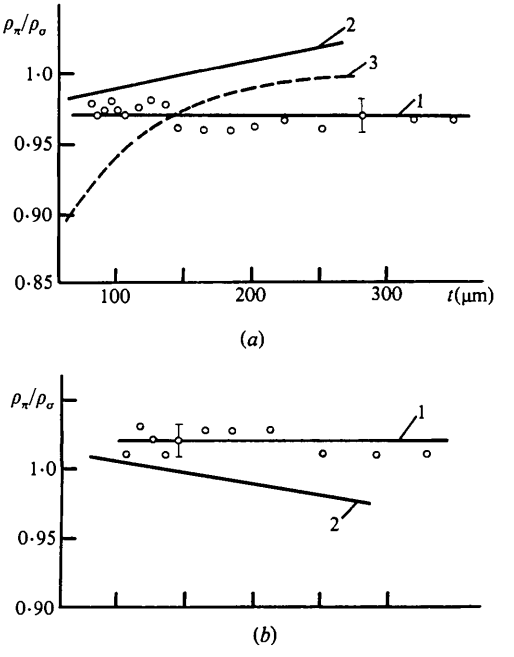

Fig. 7. Thickness dependence of the polarization ratio at dislocation density (*a*) $4{\cdot}8 \times 10^4$ and (*b*) $7{\cdot}5 \times 10^3$ mm^{-2}. (1) Experimental; (2) calculated from equation (12); (3) calculated from equation (9).

region of linear change in ln Y extends to 250 μm for reflection 111 and is below 200 μm for reflection 333. This suggests that the additional absorption coefficient of the diffracted radiation is not associated with the secondary extinction effect.

The second confirmation of this suggestion is the thickness dependence of the polarization ratio. If the secondary extinction effect took place, the polarization ratio in the linearly changing region of ln Y would be determined by the relation

$$\rho_\pi/\rho_\sigma = C^2 \frac{Y_p^\pi}{Y_p^\sigma} \exp[\alpha Q_\sigma Y_p (1 - C^2 Y_p^\pi / Y_p^\sigma) t]. \quad (12)$$

The thickness dependence of ρ_π/ρ_σ from (12) does not agree with the experimental one (Fig. 7). At $N_d = 4{\cdot}8 \times 10^4$ mm^{-2} the calculated value of ρ_π/ρ_σ increases with thickness and is over the experimental one throughout the range. It is the opposite at $N_d = 7{\cdot}5 \times 10^3$ mm^{-2}, *i.e.* the calculated polarization ratio decreases with the crystal thickness. The experiment shows that ρ_π/ρ_σ is not a factor of thickness.

Finally, the secondary extinction approach cannot explain why the measured extinction factor reaches a constant at some value of crystal thickness.

Thus, the present analysis culminates in the conclusion that the secondary extinction effect is not of major importance in X-ray diffraction in real crystals. This coincides with the conclusion from the investigations of the polarization coefficient within the Bragg reflection range (Olekhnovich & Markovich, 1978; Olekhnovich *et al.*, 1980).

In considering diffraction in low-dislocation-density crystals we proceeded from assumptions of the coherent and diffuse components, the absorption of the coherent component being due to the diffuse one. Such an approach could probably be used in diffraction analysis for high-dislocation-density crystals. It is justified by a large primary extinction effect, which is connected with coherent scattering. From that approach one can assume that the extinction factor decreasing with crystal thickness is due to coherent-wave absorption through the diffuse component. At the same time one should remember that coherent waves are limited by coherent regions in strongly distorted crystals. Then, disregarding the diffuse component, the extinction factor can be written as

$$Y = Y_p \exp(-\mu_d t/\gamma), \quad (13)$$

where Y_p is the primary extinction factor for an average coherent block, μ_d is an absorption coefficient due to the diffuse scattering. This relation is written assuming that the wave coherence of separate blocks does not change with crystal thickness.

Let us consider the variation of μ_d with the dislocation density. The value of μ_d is defined from the tilt-angle tangent of the linearly changing part of ln Y (Fig. 8). Table 1 presents the μ_d values found for the reflections 111 and 333 of all studied samples, including the samples with low dislocation density.

It is seen that the change of absorption coefficient with the dislocation density has a general regularity in the whole series of samples. μ_d is maximum for both reflections at $N_d = 7{\cdot}5 \times 10^3$ mm^{-2}. An increase or decrease in the dislocation density makes μ_d fall (Table 1). This can be explained if one bears in mind that μ_d is derived from two factors related to coherent and diffuse scattering components, respectively. The value of μ_d will be extremum at some dislocation density since the first factor decreases and the second one increases with the dislocation density.

From this approach one can account for the observed polarization-ratio dependence on crystal thickness. The absence of a distinct change of ρ_π/ρ_σ with crystal thickness is possible provided μ_d is the same for the π and σ polarizations. This condition can really exist, since the given coherent component factor is smaller for π than for σ polarization, while the diffuse component factor in contrast is larger for π polarization because of the diffuse scattering extinction (5).

Appropriate investigations are needed to make a detailed analysis of these results.

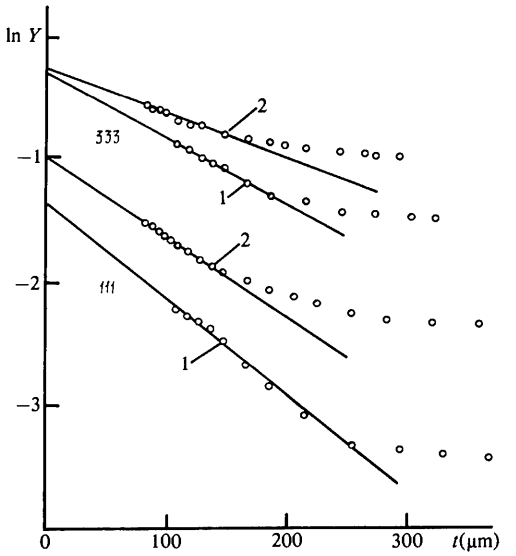

Fig. 8. ln Y *versus* crystal thickness at dislocation density (1) $7{\cdot}5 \times 10^3$ and (2) $4{\cdot}8 \times 10^4$ mm^{-2}.

Table 1. *Absorption coefficient μ_d at different dislocation densities N_d*

Sample		I	II	III	IV	V	VI
N_d (mm^{-2})		30	100	$7{\cdot}5 \times 10^3$	$4{\cdot}8 \times 10^4$	$1{\cdot}3 \times 10^5$	1×10^6
μ_d (cm^{-1})	111	—	5	75	63	35	22
	333	8·3	22·1	32·8	25·7	12	12

Table 2. *Primary extinction factor, polarization ratio and average block size at various dislocation densities*

N_d (mm^{-2})		$7{\cdot}5 \times 10^3$	$4{\cdot}8 \times 10^4$	$1{\cdot}3 \times 10^5$	10^6
Y_p		0·259	0·370	0·383	0·55
D (μm)		14·1	11·9	11·7	9·3
111	$(\rho_\pi/\rho_\sigma)_{exp}$	1·02	0·98	0·96	0·89
	$(\rho_\pi/\rho_\sigma)_{calc}$	1·02	0·97	0·93	0·88
333	$Y_{p\,exp}$	0·69	0·77	0·79	0·89
	$Y_{p\,calc}$	0·67	0·74	0·75	0·87

The primary extinction factor Y_p (13) of the average coherent block can be estimated to a first approximation from the expression obtained for a finite perfect crystal (Olekhnovich *et al.*, 1980):

$$Y_p = \exp(-\tau_c^2/4)\,\{1 + 0{\cdot}147\exp[-0{\cdot}45(\tau_c - 4{\cdot}2)^2]\}, \tag{14}$$

where $\tau_c = D/\Lambda$, D is an effective dimension of the coherent block.

The effect of anomalous transmission on the primary extinction factor for the size of blocks under study is negligible (Olekhnovich, 1979) and has not been taken into account. The D found from (14) has the same order of magnitude as an average distance between the dislocations. Using the effective block dimensions, found from Y_p for reflection 111, we estimated the polarization ratio for this reflection:

$$\rho_\pi/\rho_\sigma = C^2\,Y_p^\pi/Y_p^\sigma, \tag{15}$$

and also the factor Y_p for reflection 333 (Table 2).

In the calculations we took into account $\tau_c^\pi = C\tau_c^\sigma$, $(\tau_c\Lambda)_{111} = (\tau_c\Lambda)_{333}$. Table 2 shows that the found ρ_π/ρ_σ values agree with the experimental ones within experimental error. The estimated factor Y_p for reflection 333 is somewhat below the experimental one. This may be because the diffuse scattering contribution is not taken into account. Thus the given comparison shows that (14) can be used for the primary extinction correction in mosaic crystals.

4. Conclusion

Dislocation crystals are divided into two groups according to the character of the thickness dependence of the integrated intensity. For the first group of crystals (dislocation density below 10^3 mm^{-2}) effects of the integrated intensity thickness oscillation and the anomalous transmission are evident. The ratio of oscillation period for a perfect crystal to that of a dislocation one defines directly the Debye–Waller static factor $E = e^{-L}$. This factor decreases with the dislocation density and reflection order, though its value differs little from 1. For example, for reflection 333 it constitutes 0·97 even at a dislocation density of 100 mm^{-2}. A similar result for germanium (reflection 220) was obtained by Datsenko (1977) from the data on anomalous transmission.

For the second group of crystals (dislocation density beyond 10^3 mm^{-2}) the extinction effect is observed. Analysis of the extinction-factor thickness dependence and polarization ratio for crystals having various dislocation densities shows inapplicability of diffraction theories, based on the Darwin transfer equations.

The obtained diffraction data can be treated assuming that diffracted radiation consists of coherent and diffuse components, the coherent component being absorbed due to the diffuse scattering.

References

ALDRED, P. J. E. & HART, M. (1973). *Proc. R. Soc. London Ser. A*, **332**, 223–238.

BECKER, P. J. & COPPENS, P. (1974). *Acta Cryst.* A**30**, 129–147.

DATSENKO, L. I. (1977). *Dinamicheskoe Rasseyanie Rentgenovskikh Luchei i Strukturnoe Sovershenstvo Realnykh Kristallov Poluprovodnikov*. Thesis, Kiev.

DEDERICHS, P. H. (1970). *Phys. Rev. B*, **1**, 1306–1317.

KATO, N. (1968). *J. Appl. Phys.* **39**, 2231–2237.

KATO, N. (1980*a*). *Acta Cryst.* A**36**, 763–769.

KATO, N. (1980*b*). *Acta Cryst.* A**36**, 770–778.

KRIVOGLAZ, M. A. (1967). *Teoriya Rasseyaniya Rentgenovskikh Luchei i Teplovich Neitronov Realnimi Kristallami*. Moskva: Nauka.

LAWRENCE, J. L. & MATHIESON, A. McL. (1977). *Acta Cryst.* A**33**, 288–293.

LIDER, V. V., CHUKHOVSKII, F. N. & ROGANSKII, V. N. (1977). *Fiz. Tverd. Tela*, **19**, 1231–1237.

OLEKHNOVICH, N. M. (1979). *Izv. Akad. Nauk BSSR, Ser. Fiz. Mat. Nauk*, **5**, 88–93.

OLEKHNOVICH, N. M. & MARKOVICH, V. L. (1978). *Krystallografiya*, **23**, 658–661.

OLEKHNOVICH, N. M., MARKOVICH, V. L. & OLEKHNOVICH, A. I. (1980). *Acta Cryst.* A**36**, 989–996.

SOMENKOV, V. A., SHILSTEIN, S. SH., BELOVA, N. E. & UTEMISOV, K. (1978). *Solid State Commun.* **25**, 593–597.

TAKAGI, S. (1969). *J. Phys. Soc. Jpn*, **26**, 1239–1253.

ZACHARIASEN, W. H. (1967). *Acta Cryst.* **23**, 558–564.